Analysis of Pore Structure Effects on Diffusive Reactive Transport in Bentonite via Pore Network Models – 14068

Qingrong Xiong[1], Simon Kwong[2], Andrey P Jivkov[1]

[1] Research Centre for Radwaste & Decommissioning and Modelling & Simulation Centre, Dalton Nuclear Institute, The University of Manchester, UK.
[2] National Nuclear Laboratory, UK.

ABSTRACT

Bentonite is widely considered as one of the most suitable backfill materials for deep geological disposal of radioactive nuclear waste. In order to assess the long-term containment performance of radioactive waste repositories, good knowledge of transport behaviour of radionuclides in bentonite is required.

While it is possible to study the complex diffusion phenomena using pore network models, accurate description of the morphology of real porous media is required to support model parameterisation (i.e. pore size distribution, throat size [1] distribution and connectivity parameters). However, for bentonites with tight pore spaces that are of interest to potential geological repository applications, current experimental techniques do not allow resolution of sufficient number of throat sizes (if at all). Consequently, often only pore size distribution is available, while connectivity data, e.g. pore coordination statistics/spectra are lacking.

In order to circumvent this problem, a meso-scale model for diffusion of foreign species through porous media is proposed. The model considers diffusion as a continuum process operating on a discrete geometrical structure dictated by the pore size distribution. The effect of connectivity can be derived indirectly from macroscopically measured mass transport. Local diffusivities and hence connectivity are seen to be dependent on the size of the diffusing species and the sorption of those species onto the pore walls. As such, the bulk diffusivity of the medium can be analysed by considering the effects of pore structure alone, and in combination with sorption.

This paper presents initial results for the effects of solute sizes on the topological and physical properties of the porous network. Besides emulating the effect of sorption, the approach could in principle be extended to other pore space changing mechanisms (e.g. precipitation, dissolution, micro-cracking, etc.) for deriving mechanism-based evolution laws for the transport parameters of porous media.

[1] A standard parameter in Pore Network Model that represents the cross-sectional area of the passage links between the pore voids.

INTRODUCTION

Bentonite is commonly considered as a suitable backfill material around containers of high-level radioactive waste in most of the current designs for deep geological disposal of radioactive wastes. It is often served as a critical barrier to radionuclide transport between degrading containers and host rock over very long time scales. Bentonite typically exhibits very low permeability, has a large specific surface area, high ion-exchange capacity, and sorption affinity for organic and inorganic ions. The principal mass transport mechanism in bentonite is diffusion. It is therefore of great interest to repository designers and risk assessors to be able to predict diffusivity of radionuclides in bentonite under given evolution scenarios, particularly when the pore space could evolve over the very long time scale due to environmental factors (e.g. cement-bentonite interaction, etc.).

Pore network models are amongst the appealing approaches that have been used over years to study mass transport in porous media. These can be applied to single-phase transport problems involving relative permeability, residual saturation and capillary pressure, as well as to multi-phase flow or mass transfer problems, dispersion, etc. [1, 2, 3, 4, 5]. Pore network models idealise the medium as a set of pores, some of which are connected by throats or mass conduits, in which transport is allowed only through the system of throats. In ideal circumstances, Pore Network Model (PNM) construction requires a wide range of microstructure information, including porosity, pore size distribution, throat size distribution, average pore coordination, and the coordination spectrum: the fraction of pores coordinated by different numbers of throats [6]. For macro-porous materials the required parameters are readily obtainable with current experimental techniques, such as computed X-ray tomography [7, 8]. However, for micro- and meso-porosity, i.e. below 100 nm, the pore size distribution can usually be determined but the resolution of the experimental techniques is not sufficient to segment all the throats and calculate their sizes. For such cases, different approaches to pore network construction are required. One possibility, currently under development, is to develop a novel methodology for pore network construction for media by introduction of a physically-based length scale and to control the diffusivity of the model by the length scale. Another possibility is to assume full connectivity between neighbouring pores in a selected lattice, but to control the diffusivity of the throats through the sizes of the connected pores and the size of the solute molecules. In such way some throats remain blocked providing a specific network topology and diffusivity emerging from there [9]. This construction leads to a network length scale decided by the prescribed total porosity and the assumption that pores are located at each lattice site. In this work, the latter method will be specifically introduced.

Sorption of diffusing species changes the pore space in bentonite and may have a significant beneficial impact on the long-term diffusivity [10]. In this work we will differentiate between

the macroscopic diffusivity of the system with and without sorption [11]. The latter is usually referred to as the effective diffusivity of the medium, D_e, and depends on the pore space structure alone. The former is referred to as the apparent diffusivity, D_a, and depends on the sorption kinetics in addition to the pore space structure. A second objective of the work is to develop the model to account for sorption effects and demonstrate its use in deriving time-dependent changes in the mass transport. In view of the role of bentonite as a barrier to radionuclide transport, this study considers the diffusion of a specific U(VI) complex, $Ca_2UO_2(CO_3)_3$.. The complex (i.e. molecules of diffusing species) is selected as an illustrative radioactive waste to demonstrate the concepts of diffusion modelling using PNM. For the purpose of PNM modelling the reactive dynamics is not considered.

Rationale for modelling long term media property changes for deep geological disposal applications

As the deep repository system subjects to a variety of thermo-hydro-chemo-mechanical (THCM) effects over its long 'operational' lifespan (e.g. 0.1 to 1.0 million years), the integrity of the engineered barrier system will change over time due to a range of processes such as dissolution, precipitation, fracturing, etc.

Under typical deep repository conditions with the containment/sealing materials saturated, the bulk hydraulic conductivities of the system would be low (e.g. order of 10^{-12} to 10^{-14} m/s for dense bentonite buffer) and diffusion due to concentration gradients would be the principal mass transport mechanism. Similarly, the host rock surrounding the repository is also likely to be a diffusion dominated media. Over a very long time scale, this diffusion process could potentially allow 'release' of quantifiable contaminant into the geosphere. The containment property of the sealing system is further complicated by geochemical and thermal conditions, such as chemical zonation around waste packages; induced mineralogical changes in bentonite (e.g. dissolution and precipitation of minerals and concrete).

The extent of dissolution and precipitation would depend on many site-specific factors such as the composition of the sealing materials, the amount and chemistry of water through the media, the temperature profile of the repository system and the surrounding geosphere. Detailed knowledge of the potential influences on mass transport property (of the barrier system/media) due to these processes, broadly referred as media degradation, is therefore essential in understanding and assessing the long term containment performance of the system.

A recent modelling study [12] has examined the effects of media degradation (due to matrix porosity changes) on solute transport, under the influences of hydrogeological (diffusion dominant) and microbially mediated chemical processes. This work examines further the effects of solute size (due to sorption) on transport property (i.e. diffusion) using a meso-scale

pore network model in representing the topological and physical properties of the porous network.

The microstructure-informed modelling approach developed here provides useful insight and enables a mechanistic understanding of macroscopic processes, and the derivation of mass transport parameters and their evolution (e.g. diffusivity).

MODEL DESCRIPTION

Construction of pore network model

Pore networks can be constructed directly from reconstructed 3D-images of porous samples [13]. Such a construction uses the locations and radii of the pores and throats and results in an irregular network specific to the imaged sample. The results for transport coefficients, however, may not be representative for the material as a whole. Moreover, in the absence of data for throat locations and sizes for large class of micro- and meso-porous materials, direct construction of irregular network is not possible. One remedy is to construct a network based on a regular lattice or cellular architecture which represents the spatial distribution of pores in an average sense.

A material volume containing a set of randomly distributed pores in space can be tessellated compactly into cells using the Voronoi construction [14]. Each cell is a polyhedron containing one pore and by definition the nearest neighbours of a given pore are the pores in the cells with common faces with the given one. Assuming that mass transport through the pore space occurs between nearest neighbours, the number of outgoing throats from a pore, i.e. the pore coordination number, is given by the number of its cell's faces. To perform the initial geometric homogenisation, the regular network required is made equivalent to all possible spatial distributions of pores in a statistical sense. Based on statistical analysis of Voronoi tessellations of point sets [15], it was previously shown that the truncated octahedron, or Kelvin solid is the regular space-filling polyhedron closest to the average cell in an arbitrary spatial distribution of voids [6]. The resulting bi-regular cellular architecture offers a maximum pore coordination of 14 and the ability to tune connectivity for prescribed pore coordination spectra. The model geometry is illustrated in Fig. 1.

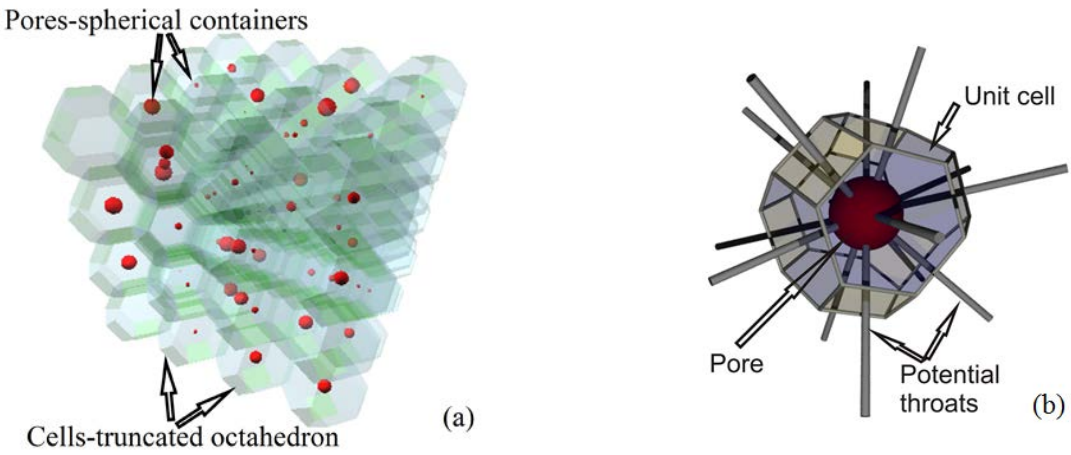

Fig.1 A segment of the cellular tessellation of 3D space is shown in Fig. 1a, together with pores of arbitrary size residing at the cell centres. A single pore in a cell is shown in Fig. 1b to emphasise that the maximum coordination of a pore in the proposed model is 14.

Compared to models based on cubic lattices with a maximum pore coordination of six, the network topology proposed in this work allows for higher pore coordination numbers [16, 17]. Further, the pore coordination spectra and the average coordination number can be generated [6] to correspond to published experimental data for macro-porous materials [18, 19]. This makes the proposed topology versatile and capable of representing large classes of porous media, with the exception of materials that possess noticeably large fractions of pores coordinated by more than fourteen pores. Since there is no experimental evidence for the existence of such materials (i.e. pore coordinate > 14) the proposed model promises to be sufficient for a wider class of porous media.

Experimental data

Bentonite clay displays pore sizes ranging from a few to several hundred nanometres [20]. In the work by Holzer et al [20], four different sample preparation techniques were tested and subsequently analysed with a number of experimental techniques to resolve pore size distribution. Of particular interest are the results obtained with high pressure frozen samples which realistically reflect the clay pore space under hydro-geological conditions. The data used in our work is the 3D pore size distribution obtained for hydrated bentonite with focused ion beam (FIB) nano-tomography. These data are presented in Fig. 2 as cumulative pore volume *versus* pore radius, revealing total porosity of the sample $\theta = 0.674$ [20]. For the construction of the pore network model, the cumulative pore volume against pore radius is converted into the cumulative probability function of pore radii, $F(r)$, using a standard statistical technique, see for example [21]. The numerically derived $F(r)$ is shown in Fig. 2 with data points shown as circular symbols. A generator of uniformly distributed random numbers $0 \leq p < 1$ can be used to

assign pore sizes. For a given random number *p*, the pore size will be $r=F^{-1}(p)$, which can be determined numerically by linear interpolation between experimental points. For the particular experimental data considered, it was found that *F(r)* can be fitted accurately with the function:

$$F(r)=\frac{1}{1+\left(\frac{r_0}{r}\right)^n} \qquad \text{(Eq. 1)}$$

where *n* defines the shape of the distribution centered over r_0 . The fit is also shown in Fig. 2. Hence, for a given uniformly distributed random number *p*, the resolved pore size is:

$$r = r_0\left(\frac{p}{1-p}\right)^{\frac{1}{n}} \qquad \text{(Eq. 2)}$$

The process defined by Eq. (2) is used to distribute pore sizes to all cells in the model. This ensures that the distributed pores follow the same size distribution as the experimentally measured population. From the volume of the distributed pores and the prescribed porosity ϕ of the system, *S*, the length-scale of a discrete network with N_c pores is determined by the formula

$$S=\sqrt[3]{\frac{2}{\phi N_c}\sum_{i=1}^{N_c}\frac{4\pi r_i^3}{3}} \qquad \text{(Eq. 3)}$$

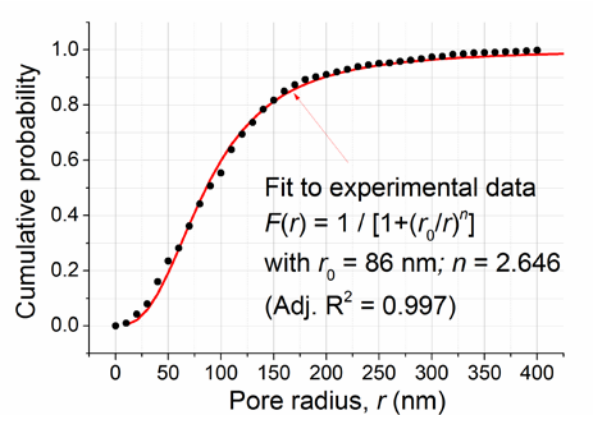

Fig. 2. Cumulative probability distribution of pore sizes in bentonite. Result obtained by converting cumulative volume versus pore radius reported in [20].

Local and global diffusivities

The driving force for local diffusion is the concentration gradient between connected pores minus the resistance provided by the throats. Although the throats are assumed not to have a

volume, they are allocated a geometrical property to assist the description of local diffusion and sorption effects. In our work, the throats are considered to be cylindrical conduits, with notional radii $R_{i,j}$, where i and j denote pore labels. The mass flow, $J_{i,j}$, through a throat is proportional to its diffusivity, $D_{i,j}$, to its cross-section area, $A_{i,j} = \pi R^2_{i,j}$, to the concentration difference between connected pores, $\Delta C_{i,j} = C_i - C_j$, and inversely proportional to its length, $L_{i,j}$, so that

$$J_{i,j} = -D_{i,j} A_{i,j} \Delta C_{i,j} / L_{i,j} \quad \text{(Eq. 4)}$$

Note that $L_{i,j}$ is the characteristic lengths between pores i and j, and can be either $L_1 = S$ or $L_2 = S\sqrt{3/2}$, depending on the throat orientation in the network structure.

In order to account for the steric hindrance and frictional resistance within the throat for diffusing species of radius r_A, the effective pore diffusivity is defined similarly to [17, 22, 23] by

$$D_{i,j} = D_0 \left(1 - \frac{r_A}{R_{i,j}}\right)^4 \quad \text{(Eq. 5)}$$

where D_0 is the free molecular diffusion coefficient of the species. To illustrate the effect of solute size, two diffusing species are considered in this work. One is a neutral U(VI) complex, $Ca_2UO_2(CO_3)_3$. The molecular size of this complex is $r_A = 0.524$ nm [11]. The other one is a hypothetical colloidal solute with $r_A = 20$ nm. The bentonite is considered fully saturated with water to reflect repository conditions, and the solutes diffuse in the water with molecular diffusion coefficients calculated with the Einstein-Stokes equation [24, 25] at room temperature: $D_0 = 4.66\times10^{-10}$ m^2/s for U(VI); and $D_0 = 1.22\times10^{-11}$ m^2/s for the colloid.

It is clear from the above setup that the mass transport of species of given size through a throat depends crucially on the decision for the hypothetical throat radius. This needs to be determined from the available information on the radii of connected pores, and throat length calculated from the prescribed porosity using Eq. (3). A benchmark for such a decision is the well-known scaling law between macroscopic diffusivity, D_m, and porosity, θ, expressed by $D_m / D_0 \sim \theta^{\beta}$. The hypothetical throat radius, $R_{i,j}$, is the same as previous work[9] and can be

$$R_{i,j} = \frac{1}{2}\left[r_i \left(\frac{r_j}{\sqrt{r_j^2 + L_{i,j}^2}} \right)^{\alpha} + r_j \left(\frac{r_i}{\sqrt{r_i^2 + L_{i,j}^2}} \right)^{\alpha} \right] \quad \text{(Eq. 6)}$$

Where α is a calibration parameter to fit a particular scaling law. The most widely applied scaling law uses $\beta = 4/3$ [19], which is reproduced with $\alpha = 1$ in our model. This value is adopted

for the rest of the work. Note that the D_m obtained with these simulations is in fact the effective diffusion coefficient of the system, D_e.

Sorption effects and apparent diffusivity

Compacted bentonite potentially offers a very high sorption capacity for radionuclides, suggesting that long-term diffusivity of such species can be significantly affected by sorption [11]. The molecules of diffusing species *M* diffuse in the pore liquid and are adsorbed onto the walls of the throat. An estimate for the effect of adsorbate obstruction on diffusivity can be obtained by reducing the radii of the throats as a function of the concentration of the diffusing species. In principle, systems with dilute adsorbate region and systems with high adsorbate concentration can be considered separately [16]. As compacted bentonite offers a very high sorption capacity for radionuclides, an estimate for the obstruction effect at high adsorbate concentration is used here. This can be obtained by considering the adsorbate to be uniformly smeared into a layer of thickness, *t*. The thickness of the adsorbed layer, *t*, can be calculated from the equation [16]:

$$t^2 - 2tR + 8\theta R r_M / 3 = 0 \qquad \text{(Eq. 7)}$$

where R is the throat radius, r_M is the radius of the diffusing species, and θ is the adsorption isotherm. The adsorption isotherm indicates how the adsorption molecules distribute between the liquid phase and the solid phase when the adsorption process reaches an equilibrium state. In this work, the Freundlich isotherm, $\theta=28.6C^{0.81}$, was adopted [25]. It should be noted here that C is the U(VI) complex in pore water. Thus, the radius of a throat after adsorption at given concentration, C_A, and hence throat radius becomes $R^*=R-t$. The flux of species *M* through a throat connecting pores *i* and *j*, with sorption taken into account is therefore given by:

$$J_{i,j} = D_0 \pi R_{i,j}^{*2} \left(1 - \frac{r_M}{R_{i,j}^*}\right)^4 \frac{C_i - C_j}{L_{i,j}} \qquad \text{(Eq. 8)}$$

This expression has been used to simulate diffusion through the system with sorption, providing an apparent diffusion coefficient, D_a. The model predictions are in very close agreement with experimental values [9]. The size of the model was smaller than the experimental test specimen and the model was solved for steady-state conditions with fixed inlet and outlet concentrations. In order to address the potential size effect, a film coefficient is introduced at the outlet boundary intended to represent model extension in the direction of diffusion. This is discussed in the next sub-section.

Film coefficients

In this study, we use a much smaller model than the realistic situation but large enough to represent the porous material properties. In order to simulate practical situations where C_1, the far-field concentration, approaches zero, a film coefficient, h, on the boundary $Z=20S$ is introduced in this study. It should be noted here that the far-field concentration is the down-stream concentration far away from the outlet surface. The film coefficient introduced in this study is used to allow for appropriate out-flux of species through the boundary $Z=20S$, so that the concentration on the outlet boundary can change with time. The film coefficient relates the flux J_m and the concentration of solute C_1 to the far-field concentration, C_∞, via $J_m=h\ (C_1-C_\infty)$. Noting that for a given C_1, the steady-state solution of the system obeys $J_m= K\ (C_0-C_1)$, where $K = D_m\ A_m / L_m$, the film coefficient can be written as a function of C_1:

$$h = K\frac{C_0 - C_1}{C_1 - C_\infty} = K\frac{1 - C_1/C_0}{C_1/C_0 - C_\infty/C_0} \qquad \text{(Eq. 9)}$$

Note that for the linear problem of diffusion without sorption, D_m and hence K is independent of the prescribed concentrations and depends solely on the pore network structure and size of diffusing species. Hence, for diffusion without sorption the film coefficient dependence on C_1 can be determined with a single steady-state solution to calculate K. For the non-linear problem of diffusion with sorption, K is a function of (C_1/C_0), which can be derived numerically by performing a number of simulations with a fixed inlet concentration, C_0, and a variable outlet concentration, C_1.

RESULTS AND DISCUSSION

The model network occupies the region ($0 \le X \le 10S$, $0 \le Y \le 10S$, $0 \le Z \le 20S$) with respect to a coordinate system (X, Y, Z) oriented along the principal directions of the unit cell. This network contains 3539 potential pores and 22006 potential throats. The size is sufficiently large to reduce the effect of the random spatial distribution of pore sizes on calculated steady-state diffusivity of the system to less than one order of magnitude. This has been confirmed by a series of random spatial distributions for which the analyses provided nearly identical results. The applied boundary conditions are: fixed concentration $C_0=5\times10^{-4}\ g/m^3$ on the boundary $Z=0$; prescribed zero flux on the boundaries $X=0$, $X=10S$, $Y=0$ and $Y=10S$; prescribed concentration C_1 or film coefficient h on the boundary $Z=20S$.

The results for the film coefficient, h, as a function of (C_1/C_0) are presented in Fig. 3. For these plots it is assumed that $C_\infty=0$. The results in Fig. 3 show how the film coefficients decrease with increase in the solute concentration at the outlet boundary. Considering transient diffusion through the pore system, the film allows for large out-flux for low outlet concentrations which

decreases with the increase of the outlet concentration. Since the solutions are obtained with identical pore distributions, the application of the film coefficient as a boundary condition represents a repetition of the same structure in the Z-direction enough times that the far-field concentration is maintained at zero. Clearly, the sorption effect is in the reduction of the film coefficient from the case without sorption. This is due to the obstructive effect of adsorbed substance, which changes local diffusivities as well as connectivity as demonstrated in the next section. The film coefficient dependencies on the concentration at the outlet boundary are used in the corresponding transient analyses.

To illustrate the effect of sorption, the change of the systems diffusivities with time is shown in Fig. 4. It is clear that the reduction of connectivity in both systems yields reductions of the long-term apparent diffusivity. In the case of U(VI) diffusion, Fig. 4a, the reduction of diffusivity is about two fold. If applied to the system with 62% porosity measured experimentally in [10] the model predicts diffusivity values closely matching the experimental values. The results of our simulations, obtained with 10 random distributions of pore sizes within the system, were in the range D_a = 2.83×10^{-12} to 2.85×10^{-11} m^2/s. Experimentally obtained values were D_a = 1.16 ×10^{-12} m^2/s to 2.30×10^{-12} m^2/s [10]. Notably, the initial apparent diffusivity of the colloidal species, Fig. 4b, is three-orders of magnitude lower than the U(VI) species, while the size of this solute is about 40 times larger. This is an illustration of the strong non-linear effect of the system connectivity. Further, the sorption reduces the diffusivity of the colloid by nearly one order of magnitude.

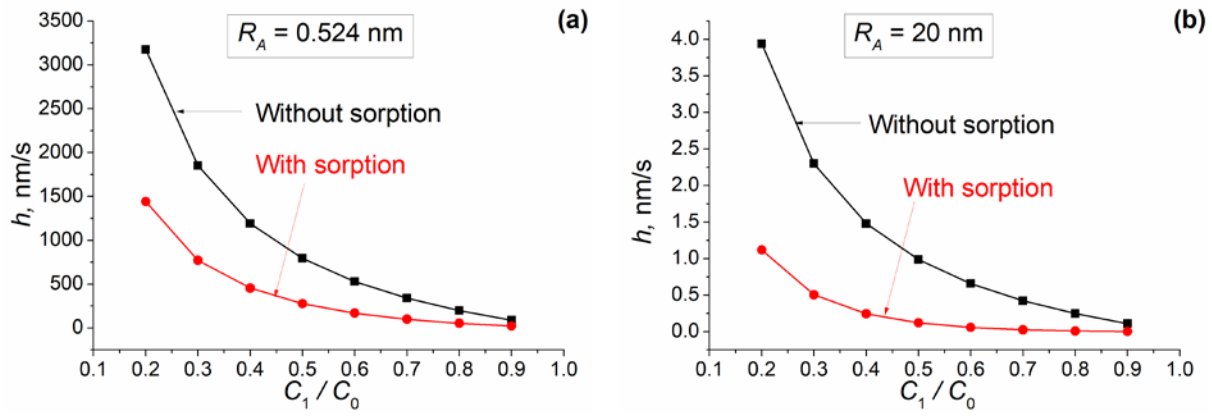

Fig. 3. Concentration dependence of the film coefficient for systems with and without sorption for selected radii of diffusing species.

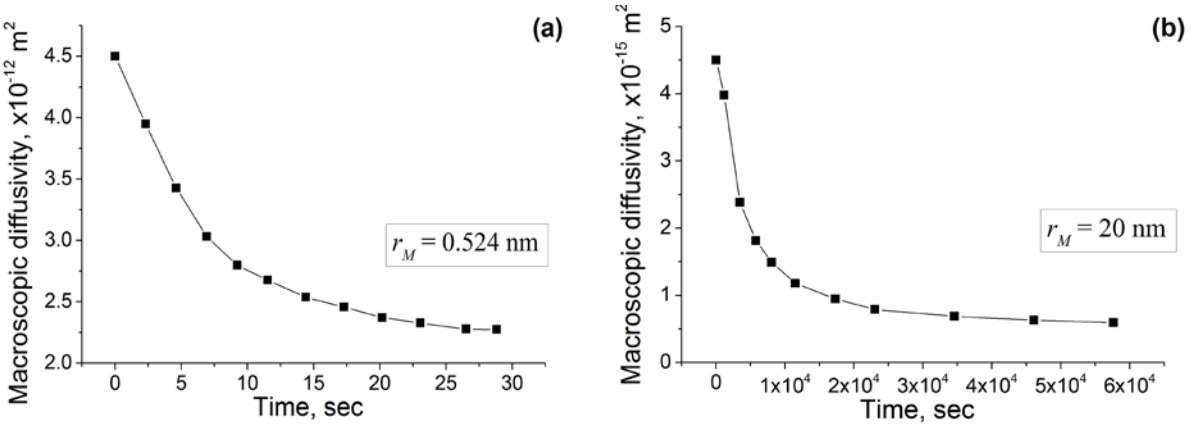

Fig. 4. Evolution of diffusivity with sorption for diffusion of U(VI)-complex (a) and colloid molecule (b).

CONCLUSIONS

The site-bond model has been developed to cover situations with unknown throat sizes and subsequently applied to bentonite using a reported experimental pore size distribution. With the combination of film boundaries and sorption kinetics the model has been shown to give macroscopic diffusivity in very close agreement with reported experimental values for radioactive contaminant with small molecular radius. Apart from the ability of the model to predict macroscopic diffusivity with good accuracy, it can provide information about the invasion of the solute in the pore system with time. This has been previously illustrated in [9], where it has been also shown how such invasion results can be used for solute transport model validation, specifically using larger solute molecules.

ACKNOWLEDGEMENTS

Q Xiong acknowledges gratefully the support of the President of The University of Manchester through the Doctoral Award Scheme. AP Jivkov acknowledges the support from EPSRC via grant EP/J019763/1, “QUBE: Quasi-Brittle fracture: a 3D experimentally-validated approach”, and from BNFL for the Research Centre for Radwaste & Decommissioning.

REFERENCES

1. BLUNT, M. J., JACKSON, M. D., PIRI, M. & VALVATNE, P. H. 2002. Detailed physics, predictive capabilities and macroscopic consequences for pore-network models of multiphase flow. *Advances in Water Resources,* 25**,** 1069-1089.
2. GAO, S., MEEGODA, J. N. & HU, L. 2012. Two methods for pore network of porous media. *International Journal for Numerical and Analytical Methods in Geomechanics,* 36**,** 1954-1970.

3. JOEKAR-NIASAR, V., HASSANIZADEH, S. M. & LEIJNSE, A. 2008. Insights into the Relationships Among Capillary Pressure, Saturation, Interfacial Area and Relative Permeability Using Pore-Network Modeling. *Transport in porous media,* 74**,** 201-219.
4. BLUNT, M. J. 2001. Flow in porous media—pore-network models and multiphase flow. *Current opinion in colloid & interface science,* 6**,** 197-207.
5. REEVES, P. C. & CELIA, M. A. 1996. A functional relationship between capillary pressure, saturation, and interfacial area as revealed by a pore-scale network model. *Water Resources Research,* 32**,** 2345-2358.
6. JIVKOV, A. P., HOLLIS, C., ETIESE, F., MCDONALD, S. A. & WITHERS, P. J. 2013. A novel architecture for pore network modelling with applications to permeability of porous media. *Journal of Hydrology*, 486, 246–258.
7. AL-RAOUSH, R. & WILLSON, C. 2005a. Extraction of physically realistic pore network properties from three-dimensional synchrotron X-ray microtomography images of unconsolidated porous media systems. *Journal of Hydrology,* 300**,** 44-64.
8. DONG, H. & BLUNT, M. 2009a. Pore-network extraction from micro-computerized-tomography images. *Physical Review E,* 80.
9. XIONG, Q., JIVKOV, A. P. & YATES, J. R. 2013. Discrete modelling of contaminant diffusion in porous media with sorption. *Microporous and Mesoporous Materials,* in press, doi: 10.1016/j.micromeso.2013.09.038
10. WANG, X., CHEN, C., ZHOU, X., TAN, X. & HU, W. 2005. Diffusion and sorption of U (VI) in compacted bentonite studied by a capillary method. *Radiochimica Acta,* 93**,** 273-278.
11. BAI, J., LIU, C. & Ball, W. 2009. Study of Sorption-Retarded U(VI) Diffusion in Hanford Silt/Clay Material. *Environ. Sci. Technol,* 43, 7706-7711.
12. KWONG, S. & JIVKOV, A.P. 2013. Diffusion Dominant Solute Transport Modelling In Deep Repository Under The Effect of Emplacement Media Degradation, Paper 13285, Proceedings of WM2013: The Waste Management Symposium 2013.
13. PIRI, M. & BLUNT, M. J. 2005. Three-dimensional mixed-wet random pore-scale network modeling of two-and three-phase flow in porous media. II. Results. *Physical Review E,* 71**,** 026302.
14. DE BERG, M., VAN KREVELD, M., OVERMARS, M. & SCHWARZKOPF, O. C. 2000. *Computational geometry*, Springer.
15. KUMAR, S., KURTZ, S. K., BANAVAR, J. R. & SHARMA, M. 1992. Properties of a three-dimensional Poisson-Voronoi tesselation: A Monte Carlo study. *Journal of Statistical Physics,* 67**,** 523-551.
16. MEYERS, J. & LIAPIS, A. 1999. Network modeling of the convective flow and diffusion of molecules adsorbing in monoliths and in porous particles packed in a chromatographic column. *Journal of Chromatography A,* 852**,** 3-23.
17. BRYNTESSON, L. M. 2002. Pore network modelling of the behaviour of a solute in chromatography media: transient and steady-state diffusion properties. *Journal of Chromatography A,* 945**,** 103-115.

18. AL-RAOUSH, R. I. & WILLSON, C. S. 2005b. Extraction of physically realistic pore network properties from three-dimensional synchrotron X-ray microtomography images of unconsolidated porous media systems. *Journal of Hydrology,* 300**,** 44-64.
19. GRATHWOHL, P. 1998. Diffusion in natural porous media. *Kluwer Academic,* London.
20. HOLZER, L., MÜNCH, B., RIZZI, M., WEPF, R., MARSCHALL, P. & GRAULE, T. 2010. 3D-microstructure analysis of hydrated bentonite with cryo-stabilized pore water. *Applied Clay Science,* 47**,** 330-342.
21. MEYER, K. & KLOBES, P. 1999. Comparison between different presentations of pore size distribution in porous materials. *Fresenius' journal of analytical chemistry,* 363**,** 174-178.
22. BRENNER, H. & ADLER, P. 1986. Transport processes in porous media. Massachusetts Inst. of Technology, Cambridge.
23. GRATHWOHL, P. 1998. Diffusion in natural porous media: contaminant transport, sorption/desorption and dissolution kinetics (POD).
24. CAPPELEZZO, M., CAPELLARI, C., PEZZIN, S. & COELHO, L. 2007. Stokes-Einstein relation for pure simple fluids. *The Journal of chemical physics,* 126**,** 224516.
25. BAI, J., LIU, C. & BALL, W. P. 2009. Study of sorption-retarded U (VI) diffusion in Hanford silt/clay material. *Environmental science & technology,* 43**,** 7706-7711.